nature portfolio

Peer Review File

Super elastic and negative triboelectric polymer matrix for high performance mechanoluminescent platforms

REVIEWER COMMENTS

Reviewer #1 (Remarks to the Author):

The field of polymer mechanoluminescence, particularly for wearable technologies, is experiencing substantial growth. This research offers a compelling alternative to conventional inorganic materials, which often lack the necessary flexibility and adaptability for dynamic mechanical environments. In this manuscript, the authors endeavor to establish a correlation between polymer elasticity and mechanoluminescence performance using a polymer matrix platform. Although the premise is both intriguing and relevant, the manuscript requires significant improvements to address several critical deficiencies. There is potential for scientific significance, but a thorough enhancement is needed for it to meet the rigorous standards and quality expected by Nature Communications. Below are several key areas that require the authors' attention:

The manuscript is deficient in its experimental section. It lacks comprehensive details on the fabrication of the polymer matrix and the experimental protocols employed, which are essential to substantiate the conclusions drawn. Clear and detailed methodology is crucial for the reproducibility of results and their validation by the scientific community.

The conclusions predominantly rely on empirical observations, with a notable absence of systematic, in-depth analysis of the structure-property relationships. This manuscript would benefit significantly from an expanded discussion on material design, particularly in how variations in chemical structure among the chosen polymers influence their interactions with ZnS particles and subsequent mechanoluminescent properties. The selection of five diverse polymers has yet to be thoroughly discussed. Each polymer could exhibit a huge range of elasticity and mechanical properties depending on the fabrication conditions. The manuscript needs to discuss how differences in chemical structure, crosslinking density, and degree of polymerization could affect the mechanoluminescence. For example, in Figure 2, the PU polymer has a similar stress-strain curve with DS and DF polymers; however, showing almost no mechanoluminescence, which need to be adequately explained. A deeper analysis of material properties and their impact on mechanoluminescence is needed.

The size and distribution of ZnS particles are also concerning. The significant size variability and irregular morphology of the particles could dramatically affect their interaction with the polymer matrix, questioning the relevance of gap size analysis presented in SEM images (Figure 4).

A 70% loading ratio of ZnS raises questions about the mechanical properties of the composites being solely attributed to the polymer matrix. Such a high concentration likely alters the

composite's overall properties, making it imperative to consider the effects of such high particle loading instead of the intrinsic properties of the pristine polymer.

The manuscript does not justify the use of un-doped ZnS. Typically, ZnS is doped with ions like Cu or Mn to enhance its mechanoluminescent properties. The rationale for using pristine ZnS should be clarified.

The parameter of transparency as used in the manuscript lacks a defined benchmark and appears to be an inadequate measure once the high load of ZnS is considered. The substantial decrease in transparency with ZnS integration should be explored more thoroughly to assess its relevance and impact.

The relationship between strain ratio and mechanoluminescence is overly simplified. It is beneficial to discuss how the observed changes in brightness relate to the activation of ZnS under stress instead of strain and the influence of particle size on sensitivity to mechanical stress.

Reviewer #2 (Remarks to the Author):

The manuscript rationales the ML process during the triboelectric process at the microscopic level with emphasis on the influence of the polymer matrix elasticity. It is shown that ML brightness is governed by the triboelectric effect generated at the interfacial pore gap. The detailed analysis at the microsopic level is inspiring and provide in-depth understanding of the ML phenomena during triboelectric processes. But the manuscript still needs to be revised to address the following issues.

(1)The curve of ER is absent in Fig. 2b.

(2)The fundamental mechano-electro-photon interaction process underlying the ML phenomenon inducing the triboelectric-induced electroluminescence model should be demonstrated.

(3)The recoverability and intensity stability of ML in the inorganic–organic composites under continuous mechanical stimulus should be investigated.

(4)The mechanical action frequency (i.e., deformation speed) could influence the ML intensity and the service life of composite materials . The dynamic aspects of the ML and the influence of frequency should be investigated.

Reviewer #3 (Remarks to the Author):

The manuscript titled “Super-elastic and negative triboelectric polymer matrix for high performance mechanoluminescent platform” unveil the role of the polymer matrix in ML platforms by using a series of elastic polymer to investigate interaction with ML brightness of copper-doped zinc sulphide microparticle. Authors systematically studied the influence of key factors of transparency, elasticity, and negative triboelectricity on the ML brightness. The rational guideline led to discovery of novel polymer matrices, polybutylene adipate-coterephthalate silane and polycarbonate silane, which not only provide high elastic performance of over 100% attributed to elasticity of polymers but also show remarkable ML brightness of 139 cd/m2 by efficient charge accumulation, which is highest brightness in extreme strain region over the 60% to date. There is an extensive amount of data provided and some interesting findings. However, the importance of negative triboelectricity on ML brightness have been widely demonstrated. For instance, in the recent reported articles (Nano Energy, 2022, 96, 107075, Nat. Commun. 2024, 15, 2673.), the positive correlation between the relative triboelectric difference between inorganic and organic phases and the ML brightness was revealed. Besides, this work only summarized the guidelines for selection of polymer matrices rather than the molecular design of polymer matrices, which weaken its instructional importance for readers. Overall, the novelty and significancy of this work is limited. It is not suitable to be published in Nature Communications.

<Point-by-Point Response to Reviewers' Comments>

Reviewer #3 (Remarks to the Author)

The manuscript titled "Super-elastic and negative triboelectric polymer matrix for high performance mechanoluminescent platform" unveil the role of the polymer matrix in ML platforms by using a series of elastic polymer to investigate interaction with ML brightness of copper-doped zinc sulphide microparticle. Authors systematically studied the influence of key factors of transparency, elasticity, and negative triboelectricity on the ML brightness. The rational guideline led to discovery of novel polymer matrices, polybutylene adipate-coterephthalate silane and polycarbonate silane, which not only provide high elastic performance of over 100% attributed to elasticity of polymers but also show remarkable ML brightness of 139 cd/m^2 by efficient charge accumulation, which is highest brightness in extreme strain region over the 60% to date. There is an extensive amount of data provided and some interesting findings. However, the importance of negative triboelectricity on ML brightness have been widely demonstrated. For instance, in the recent reported articles (*Nano Energy*, 2022, 96, 107075, *Nat. Commun.* 2024, 15, 2673.), the positive correlation between the relative triboelectric difference between inorganic and organic phases and the ML brightness was revealed. Besides, this work only summarized the guidelines for selection of polymer matrices rather than the molecular design of polymer matrices, which weaken its instructional importance for readers. Overall, the novelty and significancy of this work is limited. It is not suitable to be published in Nature Communications.

A3. Thanks for the Reviewer#3's valuable comments. In smart-wearable application field, we believe that clear guidelines for selection of polymer matrix is lacking but is required to further understand the fundamental principle between the phosphor and polymer matrix. While we agree that the role of triboelectricity on the ML process has been widely demonstrated, the attention has always been only paid to triboelectricity of two materials even though an interfacial environment of the ML platform can require other important factors like distance from phosphor as mentioned in introduction part on page 3. Furthermore, as noted by Reviewer #1, the amount of phosphor can significantly affect the elasticity of polymer and lead to a substantial change in the ML brightness due to the altered triboelectric performance in the interfacial environment (see the Q1-4 section). Therefore, to elucidate the exact correlation between the triboelectric effect and ML performance of inorganic phosphors and organic polymers for the specific target application such as wearable sensors, it is necessary to quantify

the brightness (cd/cm^2) and strain range (%) under well-defined conditions, taking into account factors such as the amount of phosphor, polymer properties, strain range, stretching and releasing speed, and even pore gaps at the single-particle level. This implies that triboelectricity is not the only factor determining ML performance, and it can be a variable that changes depending on the environment of the ML platform. Our study focuses on this viewpoint of interfacial environment enabling superior flexibility and brightness of ML platform, which is strongly affected by the polymer properties.

→ Introduction section in page 3

"While some of investigations on improving the ML performance based on polymer nature have been reported to date, most of the studies solely focused on enhancing the triboelectric effect based on negative triboelectricity despite the potential contribution of polymer elasticity. Thus, the interaction of ML performance with the fundamental parameters of the polymer has been left unexplored to date."

As mentioned in our study, other factors such as the transparency and elasticity of the polymer matrix should be considered along with triboelectricity to understand the precise mechanism and enhance the ML intensity without any loss. Firstly, the low transparency (high absorption in visible region) can cause the serious ML intensity loss of ML phosphor. As addressed in Q1-6, the ML from the ZnS:Cu must follow the light pathway through the polymer matrix to make the color emission visible to our eyes (Fig. R1b). High transmittance (> 90%) in visible region (360 ~ 780 nm) minimizes re-absorption of ML from the phosphor. It reveals that even if a polymer exhibits excellent triboelectric properties, the transparency of the pure polymer matrix must be considered to avoid ML loss from the re-absorption of polymer when selecting materials for high-luminescence mechanoluminescent platforms.

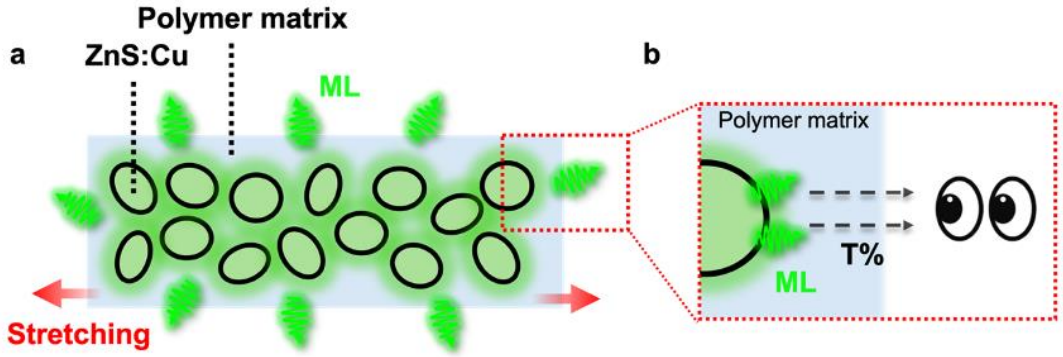

Fig. R1. a Schematic illustration of ML phenomenon of the ML platform. **b** ML light pathway through the polymer matrix from the ZnS:Cu microparticle.

Furthermore, since the triboelectric field can be defined basically as the potential difference between two areas with air as the dielectric medium, the distance between the two charged areas must be considered, as it can contribute to the magnitude of the potential difference. (E=V/d, E: electric field, V: potential difference, d: distance between two area) It is directly linked to whether the pore gap at the interfaces of the ML platform can form under the same mechanical load (Fig. 1b and Fig. 4a-d). That is, despite the polymer having high negative triboelectricity, ML cannot occur if the pore gap does not form due to the low elasticity of the polymer matrix.

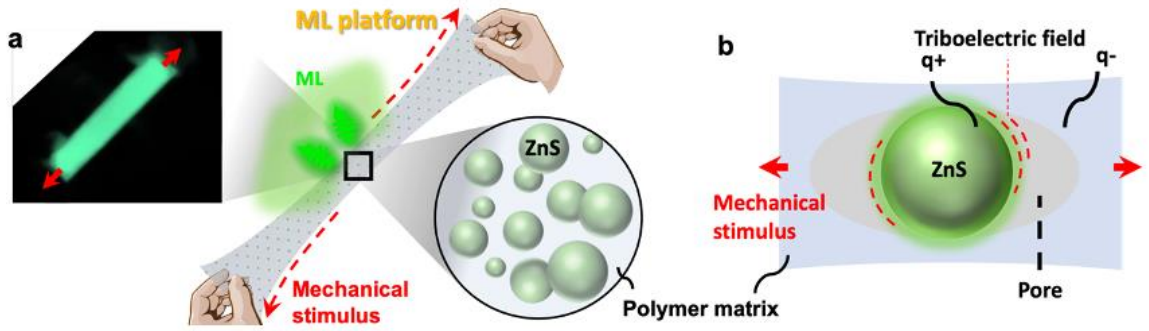

Fig. 1 a Schematic structure (inset: ML image under the stretching motion with human hands) **b** working process of the ML platform containing ZnS:Cu in the elastic polymer matrix.

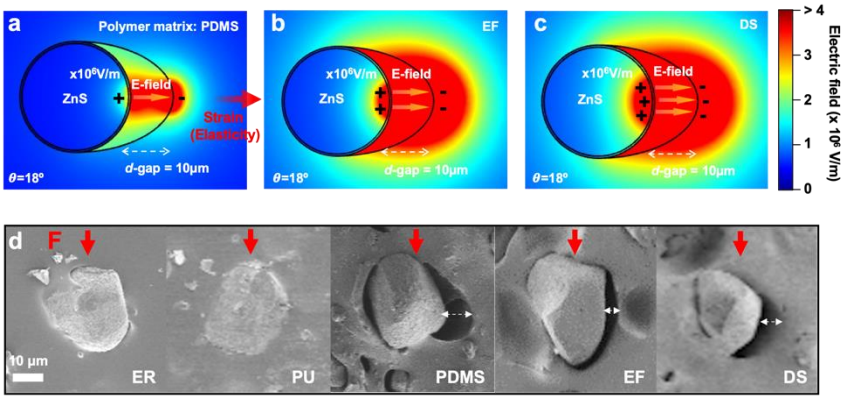

Fig. 4 FDTD simulation of the triboelectric field in the interfacial gap at 10 μm between ZnS:Cu and polymer matrix as **a** PDMS, **b** EF, and **c** DS, where the surface charge density is distributed over one-tenth of the total area (θ = 18°). **d** SEM image and **e** average d_{gap} values between ZnS:Cu single particle and each polymer matrix under the strain of 60%.

For example, in the <*Nat. Commun.*, 2024, 15, 2673> as provided by Reviewer#3, instead of a sudden triboelectric charge in contact and separation points, a gradual increase and decrease in the maximum triboelectric field is observed during the contact-separation process (Fig. R2). This validates our hypothesis that contact-separation distance can contribute to the maximum triboelectric field intensity (Fig. R2b) <*Nano Energy*, 2023, 117, 108836>. Therefore, to clearly verify the correlation between triboelectricity and ML performance, the ML performance should be explored linked with generated triboelectric field based on precise mechano-electro-luminescence process. However, In the manuscript <Nat. Commun., 2024, 15, 2673>, the correlation between the triboelectric effect and ML performance is discussed, but the influence of the distance from the phosphor is not sufficiently emphasized. Additionally, despite the significant difference (pore gap size in ML platform attributed to elasticity) in ML performance that could arise from the rigid elastic properties of silicone rubber (SC), they do not present quantified ML brightness with SC. This could obscure the fundamental measurement criteria for exploring ML performance induced by the triboelectric effect of different polymer matrices.

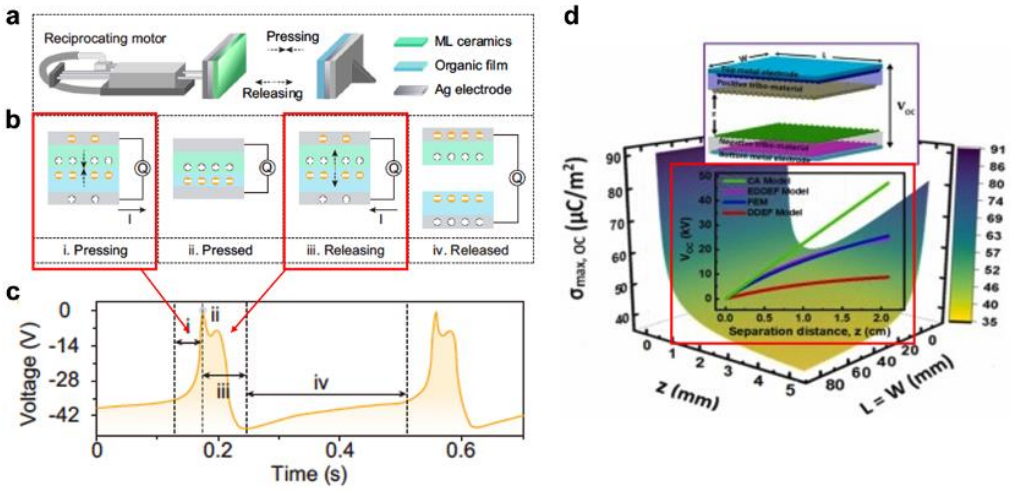

Fig. R2. a Schematic diagram of the relative triboelectric series measurement system for ML. The triboelectric charge density (TECD) between inorganic ceramics and organic filmswasmeasured to evaluate the interfacial movement between inorganic phosphors and the organic matrix in composites under mechanical actions. **b** Schematic diagrams of a full cycle of mechanical actions. The generation and transition of charges due to the coupling effect of triboelectrification and electrostatic induction (in the open-circuit mode) are depicted in the figure by using the pair of the BPC ceramic and PMDS filmas an example. **c** Changes in voltage (in V) in the pressing-releasing cycles <*Nat. Commun*. 2024, 15, 2673>. **d** Triboelectric potential of triboelectric nanogenerator depending on the contact-separation distance (z) and sample width (L) <*Nano Energy*, 2023, 117, 108836>.

In the same contexts, for the manuscript of <*Nano Energy*, 2022, 96, 107075> as raised by the reviewer, while they also suggest the relationship between triboelectricity and ML performance, the relative ML intensity is not compared between PDMS and other polymers despite different polymers being able to contribute to the activation environment of the triboelectric effect and ML performance. In Fig. R3, despite PDMS and silica gel showing no significant differences in triboelectric field and even exhibiting similar triboelectric performance under certain conditions (Fig. R3a), the ML performance visually shows a significant difference in brightness (Fig. R3b). This suggests that the elasticity of the silica gel may have interfered with triboelectric field generation by influencing pore gap formation. For an accurate correlation between triboelectricity and ML performance, identical conditions (eliminating the effects of light loss) are required, providing evidence for the justification of considering the same transparency and the formation of pore gaps due to elasticity. As proof of our concept, we

already proved that even we use the same polymer such as representative PDMS in Fig. 2b, the ML performance varies significantly depending on the strain rate. In particular, despite DS and EF exhibiting much higher triboelectricity than PDMS (Fig. 4b), the fact that their ML intensity is significantly lower than PDMS in the strain region below 60% reaffirms the fact that pore formation based on their elasticity is closely related to ML performance.

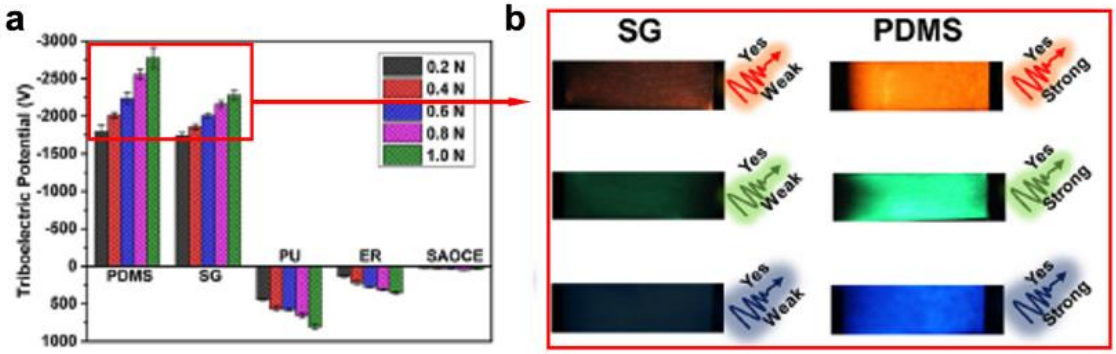

Fig. R3. a Surface triboelectric potential of the polymer matrices when rubbing with SAOCE powders for 1 min under different load conditions. **b** Illustration of the ML performance of SAOCL in various forms: powders and their composition with SG and PDMS, respectively <*Nano Energy*, 2022, 96, 107075>.

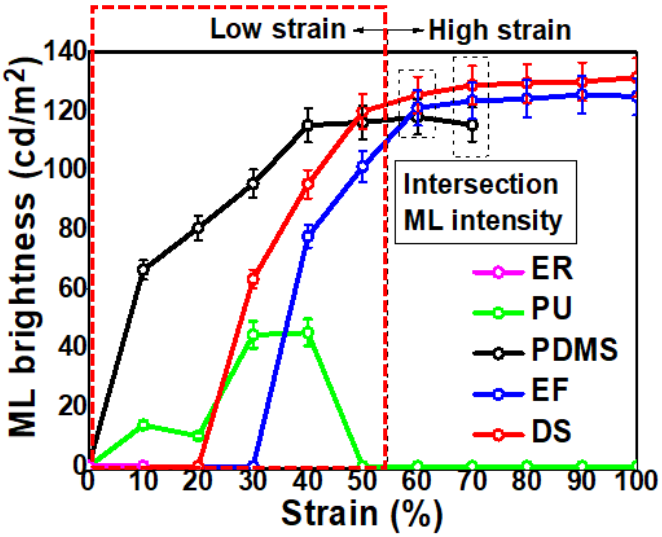

Fig. 2b ML brightness of the ML platforms by strain depending on the polymer matrices.

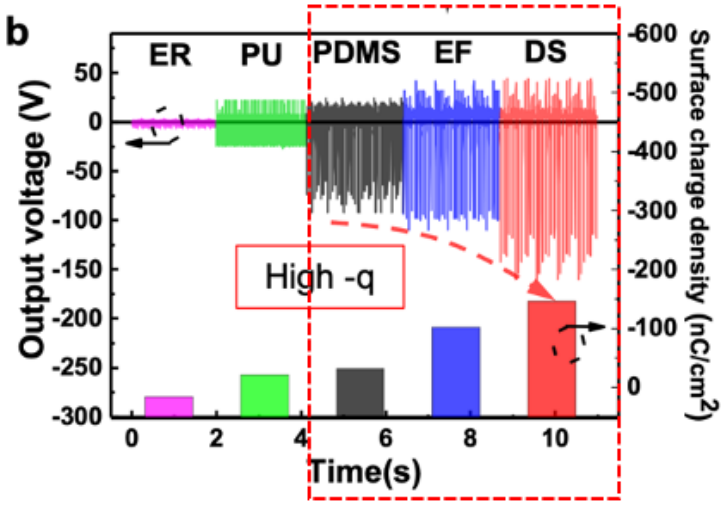

Fig. 3b The output voltage and surface charge density of the polymer matrices.

We emphasize again that we try to explore all factors of the polymer matrix to define the precise correlation with triboelectric effect, which is known to be important driving force of ML effect. In order to confirm an independent luminescence effect related solely to the influence of triboelectricity, an environment excluding transparency and elasticity must be provided. As shown in Fig. 4, we developed triboelectric field induced electroluminescence model and we confirmed the luminescence trends depending on the triboelectric effect, which is ascribed to the pure polymer matrix. As mentioned in Fig. 2b, however, luminescence trends can be significantly changed according to the strain range if elasticity is considered in a real ML environment. Therefore, we suggest again the important factors of polymer matrix should be considered to not only verify the correlation between triboelectricity and ML performance but also select the optimal materials in smart-wearable ML application, which require the optimal polymer matrix with high flexibility and rational condition for high triboelectric effect in ML platform rather than with only high triboelectricity (elasticity and high strain region).

In particular, regarding the concern of Reviwer#3 that this work only summarized the guidelines for selection of polymer matrices rather than the molecular design of polymer matrices, we carefully revised the manuscript in response to Q1-2 to further discuss chemical structure-property relationship and provide the feasibility why we selected these five types of polymer matrices for high performance ML.

(Please see the section Q1-2 below)

Reviewer #1 (Remarks to the Author)

The field of polymer mechanoluminescence, particularly for wearable technologies, is experiencing substantial growth. This research offers a compelling alternative to conventional inorganic materials, which often lack the necessary flexibility and adaptability for dynamic mechanical environments. In this manuscript, the authors endeavor to establish a correlation between polymer elasticity and mechanoluminescence performance using a polymer matrix platform. Although the premise is both intriguing and relevant, the manuscript requires significant improvements to address several critical deficiencies. There is potential for scientific significance, but a thorough enhancement is needed for it to meet the rigorous standards and quality expected by Nature Communications. Below are several key areas that require the authors' attention:

→ Thanks to Reviewer#1 for their valuable comments.

Q1-1. The manuscript is deficient in its experimental section. It lacks comprehensive details on the fabrication of the polymer matrix and the experimental protocols employed, which are essential to substantiate the conclusions drawn. Clear and detailed methodology is crucial for the reproducibility of results and their validation by the scientific community.

A1-1. We appreciate Reviewer #1's valuable comments. As requested by Reviewer #1, we added further information of materials (ML phosphor, polymers) and revised the experimental section to include more details of the fabrication protocol for all samples used in this study.

→ Revised experimental section in page 13, page 14 and highlighted in yellow.

Materials

The ZnS:Cu^{2+}@AlO_x microparticles (D502) as a main phosphor for the ML platform was purchased from Keyan Phosphor Technology Co.,Ltd. (KPT). The average particle size of the ZnS:Cu^{2+}@AlO_x was from 20 to 30 μm. For the external polymer matrices, the epoxy resin was purchased from Donyang Epoxy Co. LTD., and polydimethylsiloxane (PDMS) was purchased from the Sylgard ® 184. The polyurethane 30 (PU), Dragon skin 30 (DS), and Eco-flex 30 (EF) were purchased from the Smooth-On Inc.

Fabrication of samples

Fabrication of pure polymer film: To make the pure polymer film, we used a homemade template to ensure the film formed with dimensions of 70 mm in length, 10 mm in width, and 2

mm in thickness. All pure polymer precursors of ER, PU, PDMS, EF, and DS were poured into this template and vacuum-sealed to remove the air, then cured according to their optimal curing processes. For the ER, we used a single precursor solution and applied UV irradiation at 360 nm for 10 minutes to cure it. For the PU, EF, and DS film, we used A (main polymer solution) and B solution (curing agent) and mixed them at a 1:1 weight ratio (wt%). The mixed precursor of PU was then placed in a furnace at 80°C for 15 hour, and EF and DS precursor were placed in a furnace at 100°C for 20 minutes. For the pure PDMS film, PDMS A and B were mixed at a 9:1 weight ratio and cured in furnace at 100°C for 20 minutes. The weight ratio between main polymer solution and curing agent was used of provided condition from the company, which is considered optimal chemical reaction ratio of materials.

Fabrication of ML platform: ZnS:Cu microparticles was incorporated into each polymer precursors of ER, PU, PDMS, EF, and DS, respectively, at a weight ratio of 7:3 of ZnS:Cu microparticles:polymer matrix. The mixed composite solution with polymer matrix was poured into a homemade template (see the above context) and cured according to each method of polymer matrices following above curing condition to get an ML platform.

Fabrication of triboelectric-induced electroluminescence setup: To fabricate the triboelectric nanogenerators using pure polymer matrices of ER, PU, PDMS, EF, and DS, we prepared precursor solutions in 20 ml vials. We then used the doctor blading method to coat 2 ml of each precursor onto a 6-inch silicon wafer and follow each curing process (see the above curing method). Fabricated pure polymer films were connected with Al tape as an electrode. On the other hand, we made a ZnS:Cu single layer with PDMS between ITO electrodes (1.5 X 1.5 cm area) with a thinckness of 30 μm given the average ZnS:Cu size scale of 20-30 μm (to exclude the random characteristics caused by a thick layer) (Supplementary Fig. 12). Thereby, we successfully divide two prime parts: (1) pure polymer matrix to achieving effective triboelectricity and (2) the ZnS:Cu single layer to verify luminescence performance depending on this triboelectricity without elastic nature, and then lie on electrical connection these two parts (Supplementary Fig. 13).

Q1-2. The conclusions predominantly rely on empirical observations, with a notable absence of systematic, in-depth analysis of the structure-property relationships. This manuscript would benefit significantly from an expanded discussion on material design, particularly in how

variations in chemical structure among the chosen polymers influence their interactions with ZnS particles and subsequent mechanoluminescent properties. The selection of five diverse polymers has yet to be thoroughly discussed. Each polymer could exhibit a huge range of elasticity and mechanical properties depending on the fabrication conditions. The manuscript needs to discuss how differences in chemical structure, crosslinking density, and degree of polymerization could affect the mechanoluminescence. For example, in Figure 2, the PU polymer has a similar stress-strain curve with DS and DF polymers; however, showing almost no mechanoluminescence, which need to be adequately explained. A deeper analysis of material properties and their impact on mechanoluminescence is needed.

A1-2. Thanks for the valuable comment. We have carefully revised the manuscript on page 5 and 8 to further discuss chemical structure-property relationships and provide more explanation for why we selected these five types of polymer matrices. Since our purpose is finding a suitable polymer matrix for a human motion detection textile sensor as a smart wearable application, we preferentially considered the amorphous structure of the polymer, which provides transparency and flexibility owing to the degree of freedom of the polymer chains. As very well established in previous reports <*Polymers*, 2023, 15, 1595> <*Recent Patents on Materials Science*, 2009, 2, 171-189>, disorder of polymer chain not only prevent the light scattering in bulky matrix for transparency but also bestow free deformation durability for the elastic nature (Fig. R4).

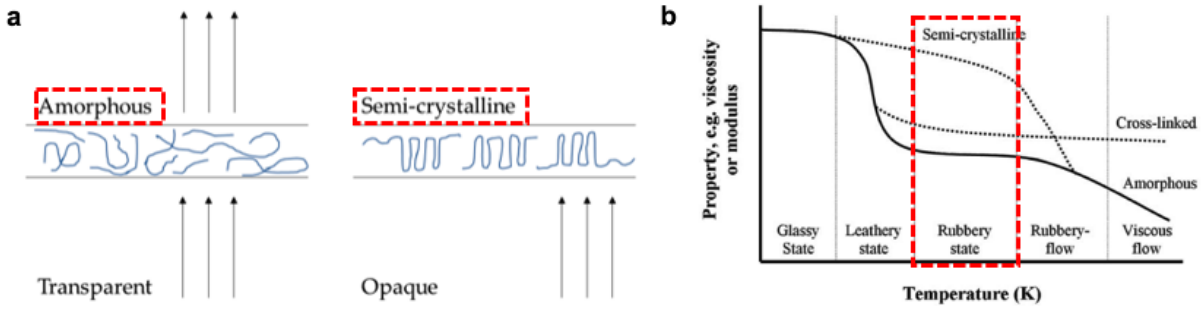

Fig. R4. a Schematic representation of the photopolymerisation process of NVCL to PNVCL in the presence of Irgacure® 2959 <*Polymers*, 2023, 15, 1595> **b** Visco-elastic regions of polymers. <*Recent Patents on Materials Science*, 2009, 2, 171-189>

We first revised the manuscript corresponding to Fig. 1d to verify amorphous structure-transparency relationships. Their high transparency over 90% as shown in Fig. 1d prove the

feasibility that their chemical structure of ER [-(CH_2-CH_2)-$_n$-(CH_2-CH(CH_3))-$_n$-(CH_2-CH=CH-CH_2)-$_n$], PU [-(R-NH-C(O)-O-R')-$_n$], PDMS [-(CH_3)$_2$SiO-]$_n$, EF [-($C_4H_8O_2$)-C(O)-C_6H_4-C(O)-O-C_4H_8-]$_n$, DS [-($C_{15}H_{16}O_2$)-($C_{16}H_{14}O_3$)]$_n$, indicate the low scattering effect and absorption in visible region. Furthermore, the XRD pattern of the ML platform in Supplementary Fig. 7, cannot exhibit any rational peak corresponding to each polymer candidate, meaning that our polymer matrices do not have sufficient crystallinity. It means that the transparent nature of each polymer provides good transmission of light through the matrix without optical loss from the ML of ZnS:Cu microparticles (further explained about this in Q1-6 section).

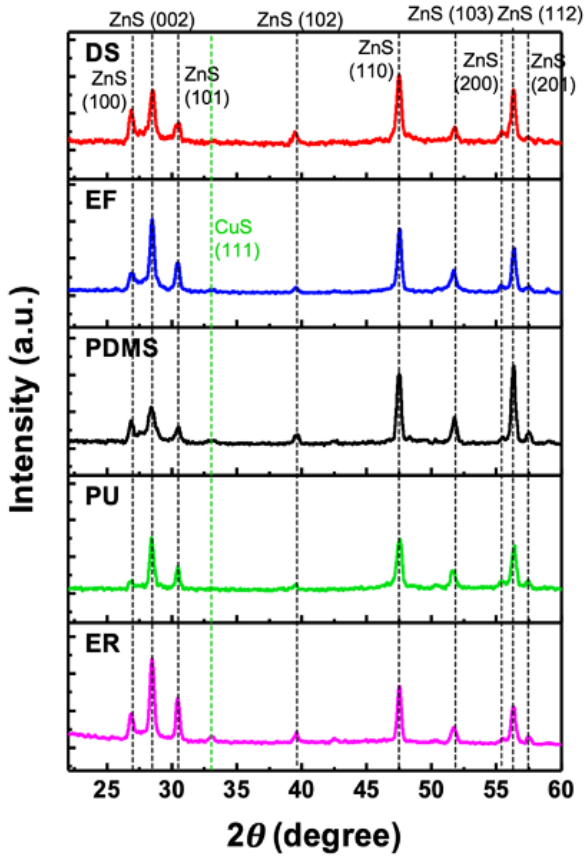

Supplementary Fig. 7 | XRD spectra of ML platform according to polymer matrix of ER, PU, PDMS, EF and DS, respectively.

→ Revised manuscript in page 5 and highlighted in yellow.

"To systematically ascertain specific factors affecting this ML effect, we screened five potential polymer matrices - ethylene propylene diene monomer rubber (epoxy resin, ER), polyurethane (PU), PDMS, EF and DS - as a candidates based on the fundamental parameters of

transparency, elasticity, and triboelectricity, which could be attributed to inherent chemical structure of monomers (Fig. 1c). We first considered the amorphous structure of the candidates to ensure maximum transparency due to the disordered polymer chain that can reduce the light scattering in the visible region compared to more crystalline analogues. We first evaluated the average visible transmittance (AVT, from 360 to 780 nm) of five selected candidates to confirm the absorption of visible range, which could decrease the ML brightness (Fig. 1d). Since the ML effect independently occurs in ZnS:Cu particles, we suggest that the high AVT values could be a crucial factor bestowing a rational light pathway without emission loss from the ZnS:Cu phosphor to human eyes."

We also now discuss the chemical structure-elasticity relationship of five candidates in manuscript corresponding to Fig. 1e (page 5). As mentioned by Reviewer#1, the elasticity of polymers is defined by their polymerization ability and the chemical structure of their monomers, and it varies depending on the degree of cross-linking. Lower cross-linking results in higher elasticity, while higher cross-linking leads to stiffer properties. In this study, however, we focused on the inherent elasticity of each polymer based on their optimal cross-linking conditions provided from the company, which is considered optimal reaction ratio between main materials and curing agent (see the revised version of experimental section in Q1-1). To clearly verify our proof of concept, we revised the strain-stress curve in Fig. 1e and focused on the yield point as a main factor of elasticity for each polymer. The elastic limit as a yield point, which is known to plays an important role in determining not only the effective flexibility but also ML effect of the ML platform to exclude ML loss unrecoverable polymer elongation, increase with the following trends against strain: ER < PU < PDMS < DS < EF on the order of strain ~%. Among all the candidates, ER exhibits the most rigid characteristics, which could be attributed to the high degree of cross-linking driven by its C=C double bonds. PU, formed by the reaction of isocyanate (-N=C=O) and polyol (-OH) groups, includes urethane bonds and displays strong intermolecular interactions, which could limit the movement of polymer chains and thus result in relatively lower elasticity. In contrast, PDMS, EF, and DS are all polymers with a siloxane (Si-O-Si) backbone, which is known to provide high flexibility due to the large bond angle and bond length of the Si-O-Si linkage, allowing for free movement of the polymer chains. The Si-O-Si bond in PDMS is much more flexible compared to carbon-based bonds (C-C, C-O, C=C), giving higher elasticity than ER and PU. In the same context, DS, which incorporates silane modification in its PDMS structure, achieves higher cross-link density,

providing greater durability and strength, while still maintaining flexibility. Lastly, EF, involving polybutylene adipate (PBA) and terephthalate-based structure, could show the highest elasticity among the Si based polymers due to its low cross-link density along with O-Si-O bond, allowing free chain movement. As shown in Fig. 4a-d, elasticity could play an important role of creating the pore gap by the mechanical stimulus, which bestows the possible environment for generating triboelectric effect in ML process.

→ Revised Fig. 1e and highlighted in yellow.

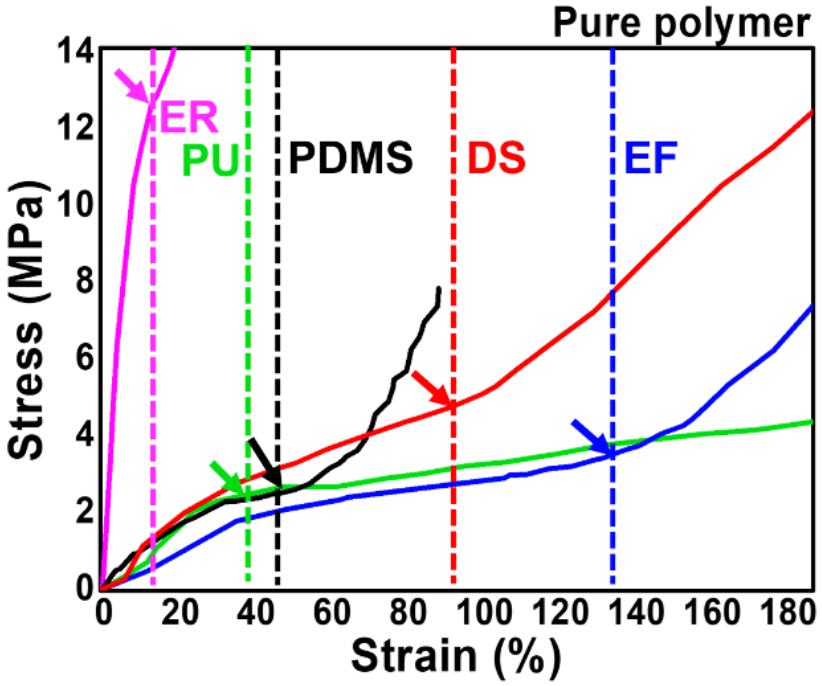

Fig. 1e Stress-strain graphs indicating the yield points of the selected polymer matrices.

→ Revised manuscript in page 5 and highlighted in yellow.

"We then considered the elasticity of our candidates, which could be defined by their polymerization ability and the chemical structure of their monomers, and it varies depending on the degree of cross-linking. Based on each chemical structure (shown in Fig. 1c), we focused on the inherent elasticity regarding each monomer under the optimal reaction ratio between main materials and curing agent (see the experimental section). To confirm the elasticity of all candidates, we accessed the analysis of strain-stress characteristics of pure polymer matrices by use of force meter (Fig. 1e) and focused on the yield point as a main factor in determining elastic nature of polymers. The evaluated strain tolerances (maximum strain range enabling full recovery to original state) increase with the following trends against stress before reaching

the failure position: ER < PU < PDMS < DS < EF on the order of strain ~% (Supplementary Fig. la, Supplementary Table 1). Additionally, the elastic limit as a yield point also exhibits the same trends, which is known to be plays an important role in determining not only the effective flexibility but also ML effect of the ML platform to exclude ML loss with unrecoverable polymer elongation. For the trend of elasticity of polymers, ER exhibits the most rigid properties, which could be attributed to the high cross-linking ability by its C=C double bonds. For PU, while the urethane bonds by means of the reaction of isocyanate (-N=C=O) and polyol (-OH) groups provide greater flexibility than ER, strong intermolecular interactions could limit the movement of polymer chains. In contrast, high yield points of PDMS, EF, and DS can be ascribed to the siloxane (Si-O-Si) backbone, which is known to provide high flexibility compared to carbon-based bonds (C-C, C-O, C=C) due to the large bond angle and length of them, allowing for free movement of the polymer chains. In particular, DS and EF stand out for their elasticity (high yield point), which can be ascribed to silane modification in DS, resulting in higher cross-linking than in PDMS, and to the polybutylene adipate (PBA) and terephthalate-based structure, along with silane groups, providing much more free movement of chains in EF, respectively."

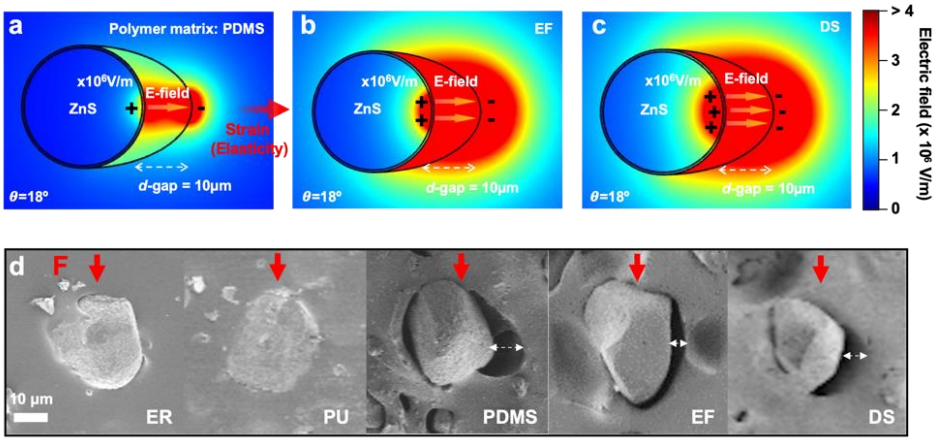

Fig. 4 FDTD simulation of the triboelectric field in the interfacial gap at 10 μm between ZnS:Cu and polymer matrix as **a** PDMS, **b** EF, and **c** DS, where the surface charge density is distributed over one-tenth of the total area (θ = 18°). **d** SEM image and **e** average d_{gap} values between ZnS:Cu single particle and each polymer matrix under the strain of 60%.

Considering the influence of polymer elasticity in providing pores, the triboelectric effect occurring within the pore gaps has been recognized as playing a crucial role in enhancing ML

performance <*ACS Appl. Mater. Interfaces,* 2019, 11, 5200−5207, *Small*, 2024, 20, 1613-6810>. The chemical structure of polymers is primarily related to their electron-withdrawing ability, which directly correlates with their triboelectricity <*Adv. Sci.* 2020, 7, 2000186>. Based on this theory, we carefully revised the manuscript on page 8 and added the information of chemical structure-triboelectricity relationship. As shown in Fig. 3b, the surface charge density of all candidates, which contributes to the effective charge accumulation by mechanical stimulus, was observed capable of the triboelectric effect on the surface of polymer. As a series of polymer matrices, the observed charge density monotonically increases with the following trend: ER < PU < PDMS < EF < DS (-15.9, -21.3, -31.9, -102.1, and -146.7 nC/cm^2), which is the basic ability of electrical charge separation in contacting surface. For the chemical factors-triboelectricity relationship, ER is a non-polar polymer with low electron affinity due to the lack of highly electronegative elements, resulting in the lowest negative surface charge density. PU, with its urethane groups and the presence of oxygen and nitrogen, has a slightly higher electron affinity than ER, leading to a moderate negative charge density. On the other hand, PDMS, with its Si-O-Si backbone, has a higher electron affinity due to the presence of oxygen, giving it a relatively higher capacity for negative charge accumulation. In the same context, EF, with ester groups and a siloxane backbone, has even greater polarity, resulting in more negative charge accumulation than PDMS. Also, DS, as a silane-modified polycarbonate with highly electronegative carbonate and siloxane groups, exhibits the highest electron affinity, leading to the highest negative surface charge density among the five polymers. We believe that our revised/added discussion provide feasibility of chemical nature-triboelectricity relationship for our polymer candidates.

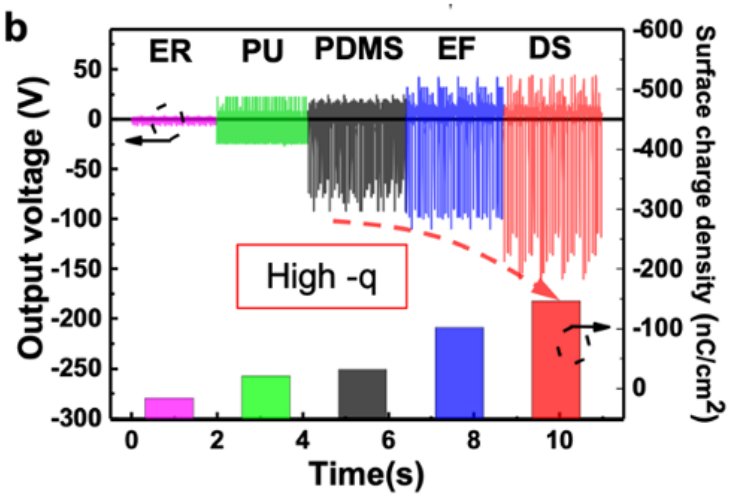

Fig. 3b The output voltage and surface charge density of the polymer matrices.

→ Revised manuscript in page 8 and highlighted in yellow.

"To define the triboelectricity, we initially evaluated the surface charge density of all candidates, which contributes to the effective charge accumulation by mechanical action, capable of the triboelectric effect on the surface of polymer (Fig 3b). As a series of polymer matrices, the observed charge density monotonically increases with the following trend: ER < PU < PDMS < EF < DS (-15.9, -21.3, -31.9, -102.1, and -146.7 nC/cm^2), which could be attributed to the electron withdrawing ability of polymers in contacting surface (Supplementary Fig. 14). For the ER, their non-polar properties could provide low electron affinity due to the lack of highly electronegative elements. However, urethane groups and the presence of oxygen and nitrogen for the PU show a higher electron affinity than ER, leading to a moderate negative charge density. On the other hand, the fact that Si-O-Si backbone (due to the presence of O) can provide higher electron affinity proves higher negative surface charge density of PDMS than ER and PU. Furthermore, EF and DS stand out for their triboelectricity, which can be attributed to the greater polarity of the ester groups in EF and the silane-modified polycarbonate groups with highly electronegative carbonate and siloxane groups in DS, respectively, enabling high electron affinity compared to the other polymer candidates. It is proved that all polymer candidates basically indicate the negatively charged surface potential by evidence with Kelvin probe force microscopy (KPFM), indicating identical trend with surface charge density (Supplementary Fig. 15)."

Based on these results, we need to collectively think about the influence of the elasticity-triboelectricity relationship for high-performance ML. We believe that this evidence is already systematically provided in our manuscript. For example, since the triboelectric field can be defined essentially as the potential difference between two areas with air as the dielectric medium, the distance between the two charged areas must be considered, as it can contribute to the magnitude of the potential difference. (E=V/d, E: electric field, V: potential difference, d: distance between two area) It is directly linked to whether the pore gap at the interfaces of the ML platform can form under the same mechanical load (Fig. 1b and Fig. 4a-d). That is, despite the polymer having high negative triboelectricity, ML cannot occur if the pore gap does not form due to the low elasticity of the polymer matrix. While PU exhibits a similar failure point to EF and DS, its yield point, a measure of the material's elastic limit, is significantly

lower than that of EF and DS. This lower yield point affects the pore formation during the ML process, ultimately limiting ML performance under high strain. We revised corresponding sentence in page 6 for better clarity.

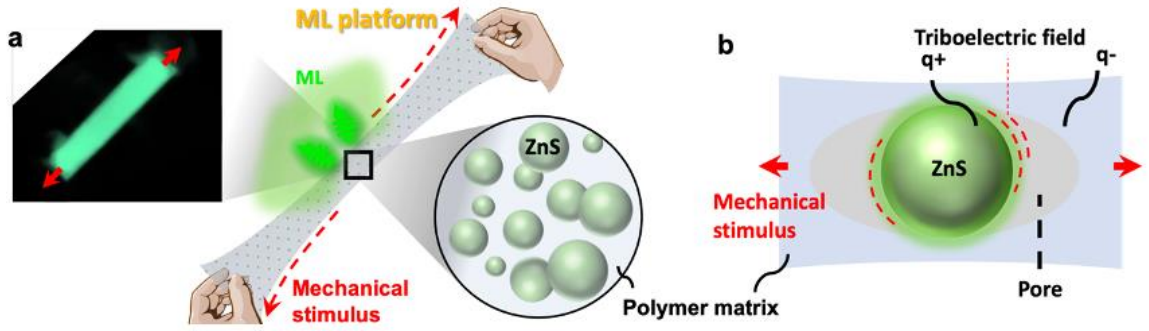

Fig. 1 a Schematic structure (inset: ML image under the stretching motion with human hands) **b** working process of the ML platform containing ZnS:Cu in the elastic polymer matrix.

→ Revised manuscript in page 6 and highlighted in yellow.

"While the failure point of PU is observed at 300% without destruction, it fails to return to its original state after exceeding a 40% stretch, meaning that the effective elasticity (yield point) of PU is only 40% under mechanical stress. This low yield point could not only interrupt the formation of the pore in the ML process (Fig. 1b) but also limits the ML performance owing to loss of elasticity when strain range is above 40%."

Q1-3. The size and distribution of ZnS particles are also concerning. The significant size variability and irregular morphology of the particles could dramatically affect their interaction with the polymer matrix, questioning the relevance of gap size analysis presented in SEM images (Figure 4).

A1-3. We appreciate Reviewer#1's valuable comment. We'd like to emphasize that we exploit the commercial ZnS:Cu microparticle (Keyan Phosphor Technology Co.,Ltd. (KPT)) with average particle size from 20 to 30 μm as written in experimental section. To further provide the feasibility of the gap size between the ZnS:Cu microparticles and polymer matrix in single particle level, we already considered the possibility of the d_{gap} with various shape and size as shown in Supplementary Fig. 11 and 19, and presented it in Fig. 4e. Based on this analysis in SEM image in supplementary figures, we used the average gap size and present representative SEM image in Fig. 4d, which can show average image of ZnS:Cu particles. To address this

concern about the irregularity of the size distribution in the polymer matrix, we added the scale values in all SEM images and revised the corresponding sentence in the manuscript to clearly inform that our d_{gap} values represent the average size. In particular, we re-emphasize our evidence that the ML performance of ZnS:Cu single particles exhibit the same trends compared with bulk films of ML platform that basically considers the irregularity of particles. As shown in Fig. R5, ML intensity of bulk film, which is reflected irregularity of randomly distributed particles, follows the same trend as the single particle scale as following: ER < PU < PDMS < EF < DS, meaning that our hypothesis in single particle level rationalize the ML trend of overall ML platforms.

→ Revised experimental section in page 13 regarding the information of ZnS:Cu purchase and highlighted in yellow.

"The ZnS:Cu^{2+}@AlO_x microparticles as a main phosphor for the ML platform was purchased from Keyan Phosphor Technology Co.,Ltd. (KPT). The average particle size of the ZnS:Cu^{2+}@AlO_x was from 20 to 30 μm."

→ Added scale values in Supplementary Fig. 11 and 19.

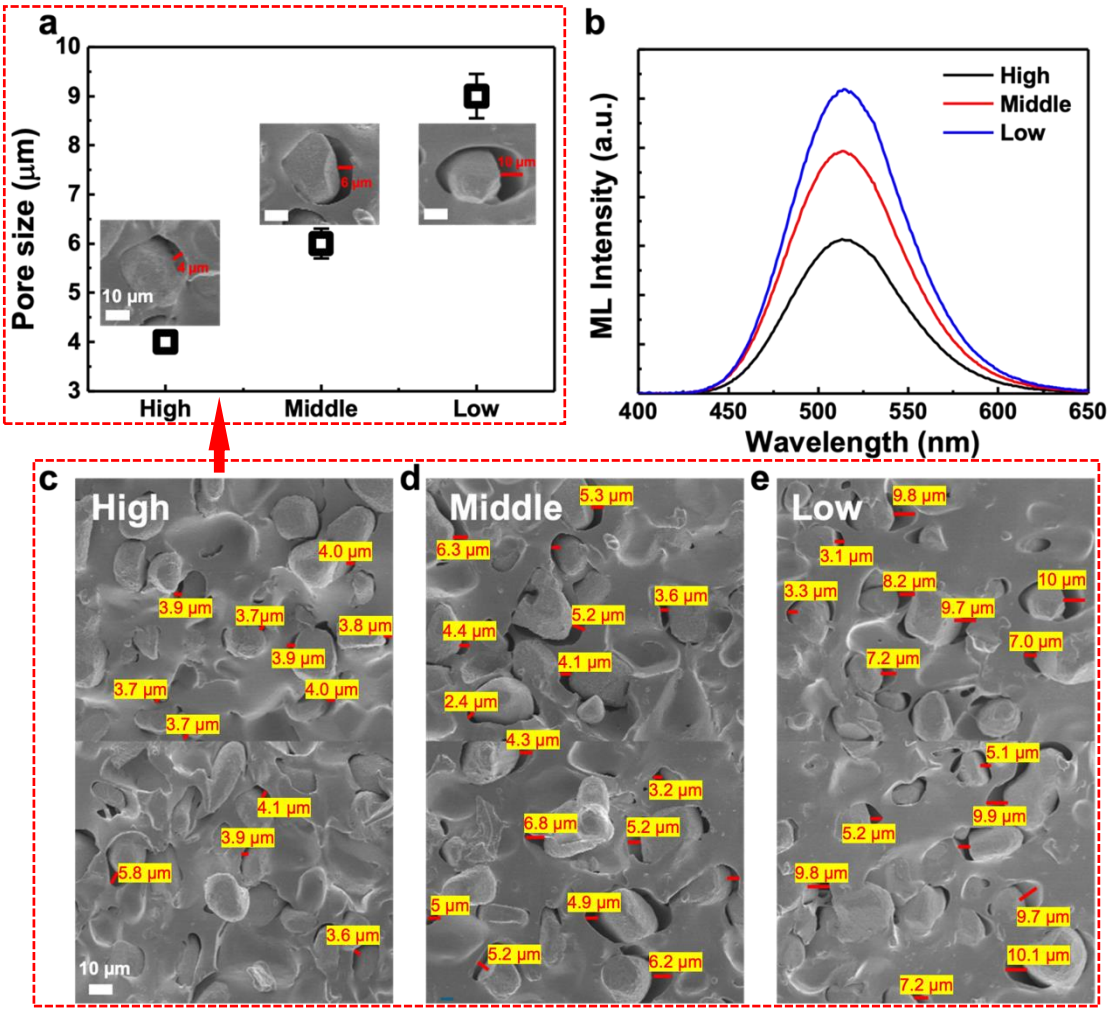

Supplementary Fig. 11 | a Average pore size, and **b** relative ML intensity of ML platforms according to PDMS elasticity. **c** Cross-sectional SEM image of ZnS in the PDMS matrix showing the average pore size depending on the elasticity.

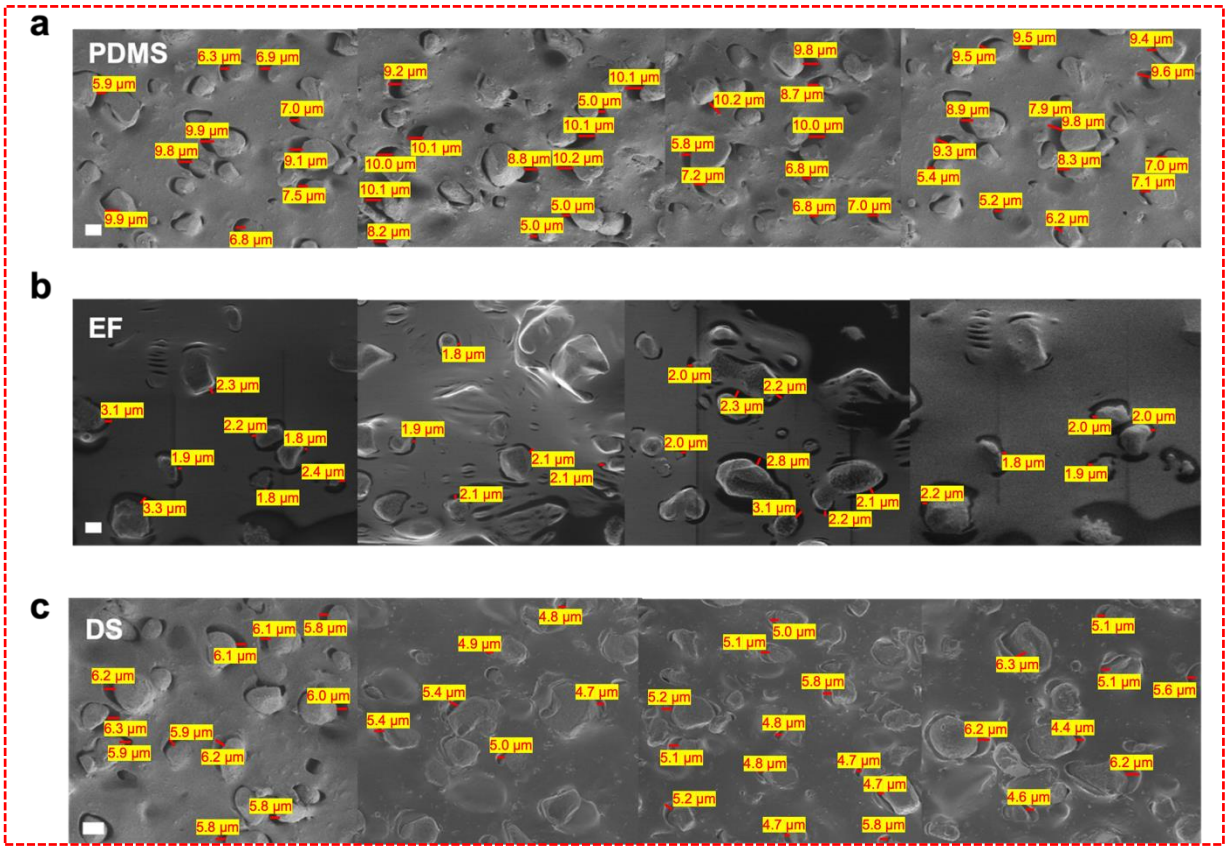

Supplementary Fig. 19 | Cross-sectional SEM image of the ML platform depending on the polymer matrix of **a** PDMS, **b** EF and **c** DS, respectively, under the same stretching motion. (bar size:10μm)

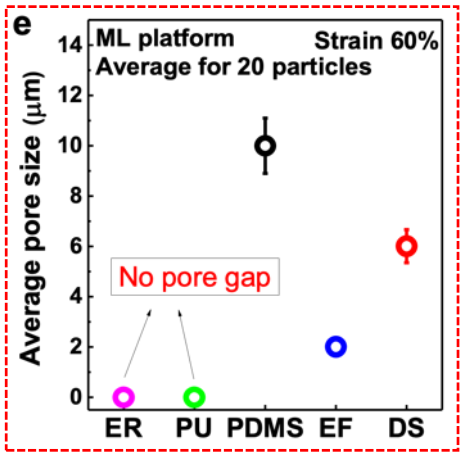

Fig. 4e Average d_{gap} values between ZnS:Cu single particle and each polymer matrix under the strain of 60%.

→ Revised manuscript regarding the Supplementary Fig. 11 in page 7 and highlighted in yellow.

"Given all samples are under identical strain conditions, we confirmed that higher elasticity corresponds to lower ML brightness due to the ability to form pores (average values of pore gap with more than 20 particles) between ZnS:Cu and PDMS, which is attributed to elasticity (low elasticity – large pore gap size, high elasticity – small pore gap size), as shown in Supplementary Fig. 11a and b."

→ Revised manuscript regarding the Supplementary Fig. 19 in page 11 and highlighted in yellow.

"We first performed an SEM analysis to assess the average d_{gap} in ML platforms with PDMS, EF and DS under the 60% strain (Fig. 4d). As expected, while we cannot identify available d_{gap} in ER and PU owing to poor elasticity (rigid feature), other candidates manifest clear d_{gap} in interface depending on their elasticity tendency: PDMS < DS < EF (average d_{gap} with more than 20 particles: 10, 6, and 2 μm, respectively), proving our hypothesis that elasticity contributes to d_{gap} (Fig. 4e, Supplementary Fig. 19)."

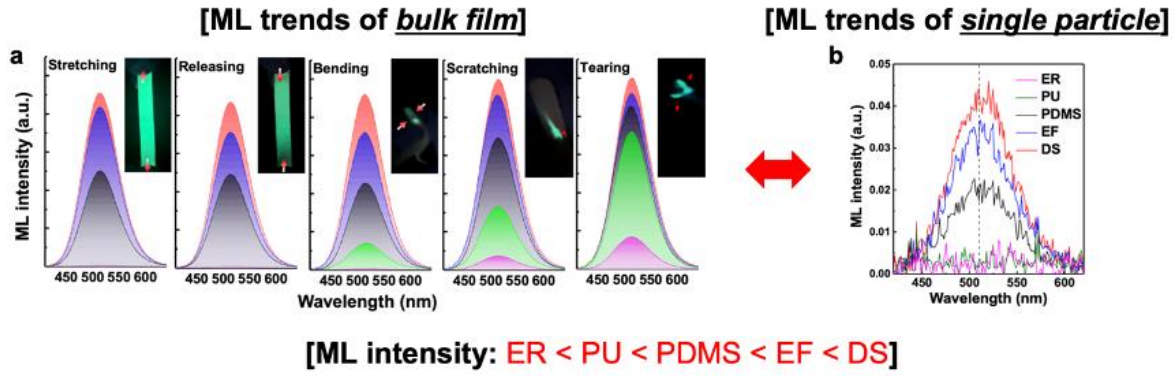

Fig. R5. ML intensity of **a** bulk film and **b** single particle in ML platform depending on the polymer matrices. ML intensity in **a** was confirmed considering various mechanical stimulus involving the stretching, releasing, bending, scratching, and tearing.

Q1-4. A 70% loading ratio of ZnS raises questions about the mechanical properties of the composites being solely attributed to the polymer matrix. Such a high concentration likely alters the composite's overall properties, making it imperative to consider the effects of such high particle loading instead of the intrinsic properties of the pristine polymer.

A1-4. Thanks for valuable comment. Based on this comment, we carefully revised the

manuscript on page 6 to provide clearer understanding for readers. Furthermore, we confirmed the elasticity and brightness of ML platform depending on the loading ratio of ZnS:Cu and revised in Supplementary Fig. 9. Indeed, the overall elasticity of ML platform, which should be bestowed by polymer property, can be regulated physically according to the concentration of ZnS:Cu microparticles. Since the ZnS:Cu microparticles play a role of main emitter, the amount of ZnS:Cu (loading ratio) also determines the total ML brightness of the bulk film. As shown in Supplementary Fig. 9a, we added the elasticity of all ML platforms, which decreases according to the loading ratio from 0% to 80% due to the physical reduction of the polymer volume in the global system. Furthermore, to optimize the suitable loading ratio between ZnS:Cu and polymer matrix for ML performance, we added the ML intensity depending on the ZnS:Cu contents in Supplementary Fig. 9b. As a normal condition of ML effect at 60% strain, while ER and PU cannot exhibit the effective ML due to their poor elasticity, increasing trends of ML intensity from 10% to 70% can be observed in PDMS, EF, and DS, respectively. However, the 80% loading ratio indicates ML degradation, which can be attributed to polymer damage caused by the excessively high content of ZnS:Cu in the polymer matrix. In conclusion, the loading ratio of ZnS:Cu can primarily impact elasticity of ML platform by physically reducing the polymer content. This affects the flexibility of the ML platform, and since lower loading amounts of ZnS:Cu below 70% result in reduced brightness, as well as higher loading amounts above 70% can cause the ML degradation due to the polymer damage, we determined the most optimal ratio of ZnS:Cu to polymer at the 7:3 wt%.

→ Revised manuscript in page 6 and highlighted in yellow.

"Based on the above results, we accessed the strain tolerances for determining the elasticity of ML platforms incorporating ZnS:Cu microparticles. To determine the optimal amount of ZnS:Cu in polymer matrix, we preferentially confirm the elasticity-ML relationship depending on the weight ratio of ZnS:Cu (Supplementary Fig. 9, Supplementary Table 2). Indeed, the overall elasticity of the ML platform, which should be bestowed by the polymer property, was regulated physically according to the loading ratio of ZnS:Cu microparticles. Furthermore, since the ZnS:Cu microparticles play a role of the main emitter, the amount of ZnS:Cu particles (loading ratio) also determines the total ML brightness. As shown in Supplementary Fig. 9a, the elasticity of all ML platforms decreases according to the loading ratio from 0% to 80% due to the physical reduction of the the polymer volume in the global system. To optimize the suitable loading ratio between ZnS:Cu and polymer matrix for ML performance, we evaluated

the ML intensity depending on the ZnS:Cu content (Supplementary Fig. 9b). As a normal condition of ML at 60% strain, while ER and PU cannot exhibit effective ML due to their poor elasticity, increasing trends of ML intensity from 10% to 70% can be observed in PDMS, EF, and DS, respectively. However, the 80% loading ratio indicates ML degradation, which can be attributed to polymer damage caused by the excessively high content of ZnS:Cu in the polymer matrix. This proves that the 70% of ZnS:Cu in polymer matrix is a suitable condition for the highest ML performance. From this optimal condition, we accessed strain-stress characteristics of ML platform."

→ Added Supplementary Fig. 9 in page 11 and highlighted in yellow.

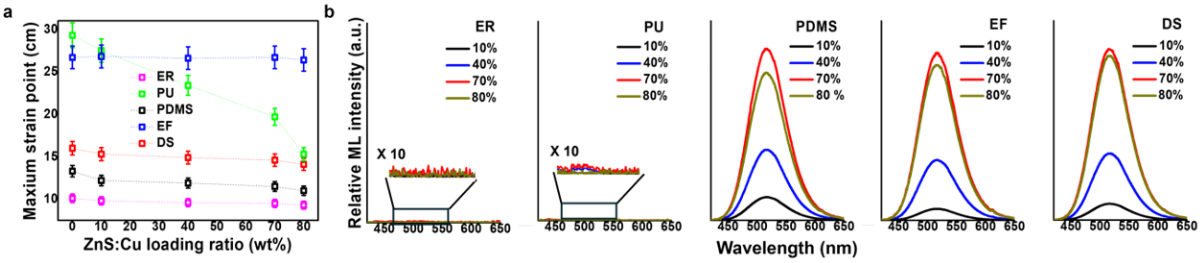

Supplementary Fig. 9. a Maximum strain point and **b** relative ML intensity of the ML platform with each polymer matrix depending on the ZnS:Cu loading ratio (wt%).

→ Added Supplementary Table 2 in page 12 and highlighted in yellow.

Supplementary Table 2. Maximum strain values of ML platform depending on the ZnS:Cu loading ratio (wt%).

ZnS loading ratio (wt%)	0	10	40	70	80
	Maximum strain (cm)				
ER	10.1	9.8	9.6	9.5	9.3
PU	29.3	27.5	23.4	19.7	15.3
PDMS	13.3	12.2	11.9	11.5	11.0
EF	26.7	26.8	26.6	26.7	26.4
DS	16	15.3	14.9	14.6	14.1

Q1-5. The manuscript does not justify the use of un-doped ZnS. Typically, ZnS is doped with ions like Cu or Mn to enhance its mechanoluminescent properties. The rationale for using

pristine ZnS should be clarified.

A1-5. Thanks for the comment. Please find the sentence of introduction part (page 4, line 85). We do not use a pure ZnS, and we denoted to ZnS from the ZnS:Cu^{2+}@AlOx. In order not to confuse the readers, we revised all these wording to ZnS:Cu instead of ZnS in this manuscript.

→ Corresponding sentence in page 4, line 85.

"Here, by exploiting a series of five elastic polymer matrices, we shed light on the principle of interaction between the ML brightness of ZnS:Cu^{2+}@AlOx microparticle (denoted of ZnS:Cu) and individually screened fundamental parameters such as elasticity and triboelectricity."

Q1-6. The parameter of transparency as used in the manuscript lacks a defined benchmark and appears to be an inadequate measure once the high load of ZnS is considered. The substantial decrease in transparency with ZnS integration should be explored more thoroughly to assess its relevance and impact.

A1-6. We appreciate Reviewer#1's comment. We'd like to say that the reason why we measured transparency of the polymer matrix is not to confirm the transmittance of the ML platform. To provide more understanding of our concept, we provided Fig. R1 and revised the sentence in manuscript to explain the role of transparency of the polymers in page 5. The transmittance of the polymer matrix plays an important role in dictating the pathway of light created from the ZnS:Cu microparticles. As shown in Fig. R1, the ML from the ZnS:Cu must transmit through the polymer matrix to make the color emission visible to our eyes (Fig. R1b). Therefore, we want to emphasize once again that it is not the transparency of the ML platform film that is important, but the transparency of the pure polymer. Furthermore, as shown in Fig. 1d, high transmittance (> 90%) of all candidates in visible region (360 ~ 780 nm) shows that ML can be emitted out of a polymer matrix with only small light loss, meaning that re-absorption of ML (510 nm emission) in polymer matrix can be excluded. It reveals that the high transmittance of the pure polymer matrix is rational to select the materials for the high brightness ML platform.

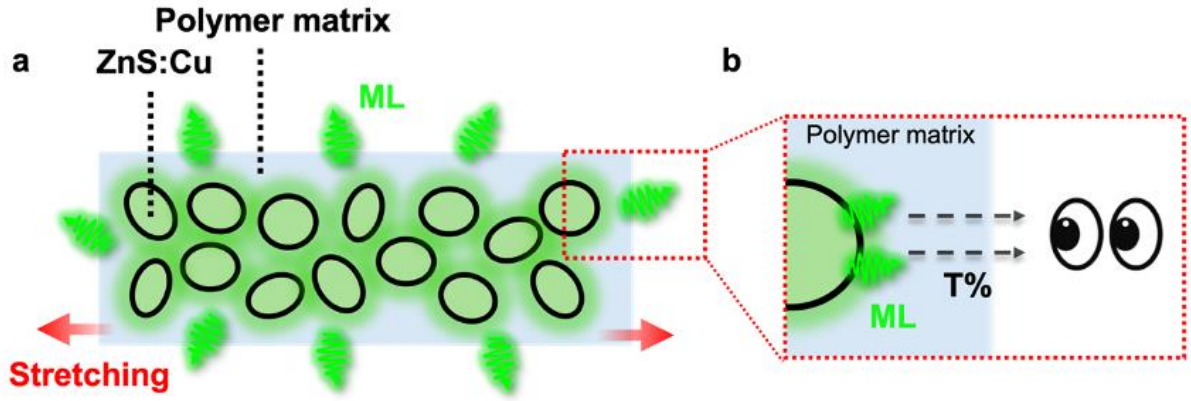

Fig. R1. a Schematic illustration of ML phenomenon of the ML platform. **b** ML light pathway through the polymer matrix from the ZnS:Cu microparticle.

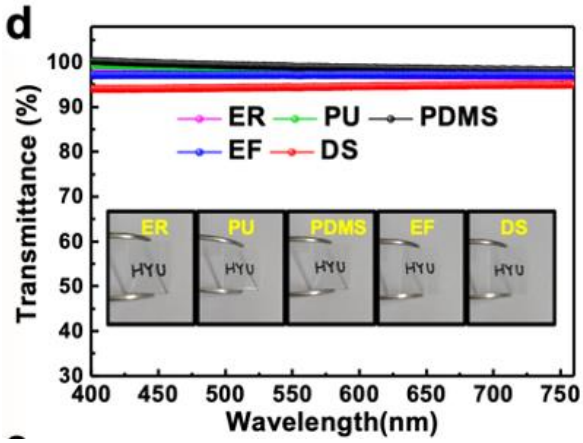

Fig. 1d Transmittance and **e** stress-strain graphs of the selected polymer matrices. The inset photo in **d** exhibits the superior transmittance of all polymer candidates by clearly identifying the word "HYU".

→ Revised the manuscript in page 5 and highlighted in yellow.

"We first evaluated the average visible transmittance (AVT, from 360 to 780 nm) of five selected candidates to confirm the absorption of visible range, which could decrease the ML brightness (Fig. 1d). Since the ML effect independently occurs in ZnS:Cu particles, we suggest that the high AVT values could be a crucial factor bestowing a rational light pathway without emission loss from the ZnS:Cu phosphor to human eyes."

Q1-7. The relationship between strain ratio and mechanoluminescence is overly simplified. It is beneficial to discuss how the observed changes in brightness relate to the activation of ZnS

under stress instead of strain and the influence of particle size on sensitivity to mechanical stress.

A1-7. We appreciate Reviewer#1's valuable comment. We'd like to emphasize again that our application is the human motion detection textile sensor, which mainly require the stretching motion by means of the human movement rather than direct force as a stress. Furthermore, in the ML platform, both stress and strain can lead to the formation of surface pores. Although ZnS:Cu is a good material capable of emitting light under direct force, in the ML platform, the direct force applied to it by the polymer is limited, following a triboelectric-induced electroluminescence process in principle (Fig. R6, please find the response of Q2-2). Therefore, we propose that whether stress or strain is applied, the size of the surface pore gaps-triboelectric relationship can determine ML performance. Based on this, we have already provided relevant results in Fig 2 b and c.

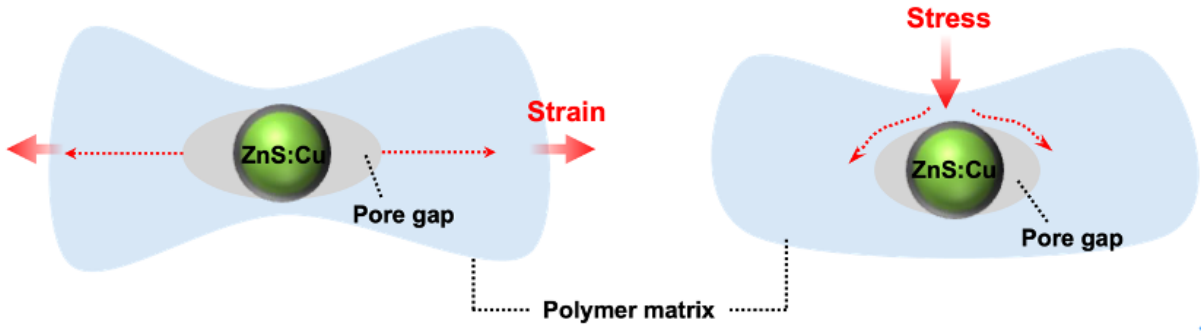

Fig. R6. Schematic of forming the pore gap in ML platform under the strain and stress as a mechanical stimulus.

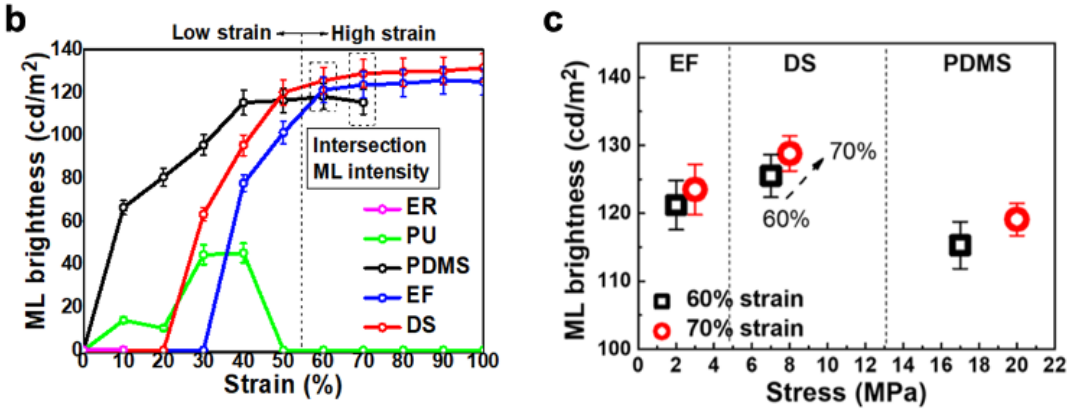

Fig. 2 b ML brightness of the ML platforms by strain depending on the polymer matrices. **c** ML brightness by stress depending on the PDMS, EF, and DS, respectively, at 60% and 70%

strain for PDMS, EF, and DS.

→ Corresponding text in manuscript on page 7.

“From these results, we then estimated ML brightness based on both strain and stress to access its relationship with elasticity as shown in Fig. 2b. As trends of elasticity, the ML platforms with ER and PU are limited effective ML across the entire strain region attributed to poorly elastic region. It strongly demonstrates that the absence of elasticity of pure polymer matrices results in weaker ML brightness of the ML platform. As shown in Fig. 2b, while EU cannot generate any ML due to the lowest elasticity, PU still show short-term ML in the effective elastic region in 40% strain, even though lead to rapid ML failure due to polymer damage.[29] In contrast, PDMS, EF and DS exhibit the increasing tendency of ML brightness in their effective elastic region owing to outstanding elasticity of polymer matrix. We note that ML brightness of PDMS can increase before the 40% strain, but eventually tends to saturate or decrease owing to a shorter yield point around 45%, as a result of polymer damage. In the same context, the ML brightness of EF and DS also monotonically increases in their effective elastic region before reaching the yield point around 100% strain, as well as continuously enhanced brightness, even surpassing PDMS beyond 60% strain. This result implies that ML platforms with PDMS, EF, and DS provide not only longer effective elastic region for ML effect but also possibility of ML process before reaching the yield point of polymer matrix, attributed to their excellent elasticity. Furthermore, ML platforms with EF and DS not only exhibited high strains of 60% and 70% at relatively low stress levels, ranging from 1 to 3 MPa and 6 to 8 MPa, respectively (Fig. 2c), but also achieve the highest ML brightness at the 70% strain with values of 119, 124, and 139 cd/m² (Fig. 2d, e).”

Reviewer #2 (Remarks to the Author)

The manuscript rationales the ML process during the triboelectric process at the microscopic level with emphasis on the influence of the polymer matrix elasticity. It is shown that ML brightness is governed by the triboelectric effect generated at the interfacial pore gap. The detailed analysis at the microscopic level is inspiring and provide in-depth understanding of the ML phenomena during triboelectric processes. But the manuscript still needs to be revised to address the following issues.

→ We appreciate Reviwer#2's valuable comment.

Q2-1. The curve of ER is absent in Fig. 2b.

A2-1. Thanks for the comment. As requested from Reviewer#2, we revised the plot to ensure that the curve of ER is clearly indicated. In the case of ER, due to the rapid degradation of the polymer, ML induced by strain and stress is not continuously sustained, resulting in an intensity close to zero. We explain this ER curve and its emission performance in the manuscript.

→ Revised Fig. 2b for the ER curve.

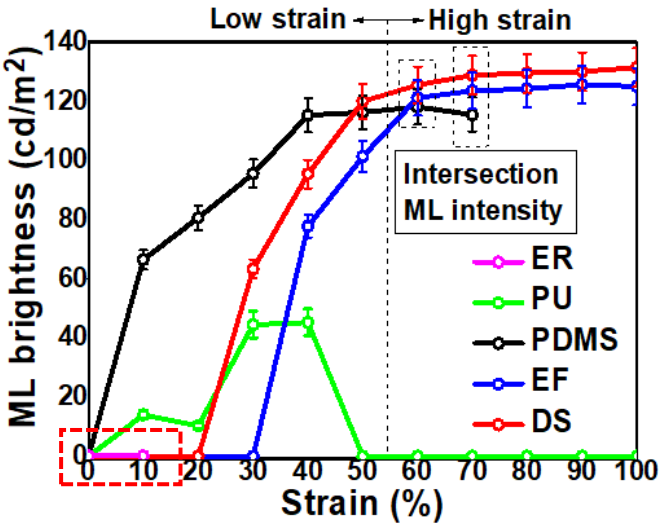

Fig. 2b ML brightness of the ML platforms by strain depending on the polymer matrices.

→ Corresponding sentence in manuscript at page 7, Line 203.

"As trends of elasticity, the ML platforms with ER and PU are limited effective ML across the entire strain region attributed to poorly elastic region. It strongly demonstrates that the absence of elasticity of pure polymer matrices results in weaker ML brightness of the ML platform. As

shown in Fig. 2b, while EU cannot generate any ML due to the lowest elasticity, PU still show short-term ML in the effective elastic region in 40% strain, even though lead to rapid ML failure due to polymer damage.[29]"

Q2-2. The fundamental mechano-electro-photon interaction process underlying the ML phenomenon inducing the triboelectric-induced electroluminescence model should be demonstrated.

A2-2. Thanks for the valuable comment. We believe that mechano-electro-photon interaction of ML platform (Fig. 1b) by means of the triboelectric effect is already proved in Fig. 3a-c as a triboelectric-induced electroluminescence model of ZnS:Cu, attributed to the mechano-electro conversion process (triboelectric effect) from the pure polymer matrices. Basically, the ML process of the ML platform can be explained by the triboelectric effect in pore gap, which should be created between ZnS:Cu and polymer matrix as shown in Fig. 1b and Fig. R7 <*ACS Appl. Mater. Interfaces,* 2019, 11, 5200−5207, *Small*, 2024, 20, 1613-6810>. It means that the electric field can induce the luminescence of ZnS:Cu microparticle by means of the triboelectric effect in pore gap. To clarify each process of both mechano-to-electro and electro-to-photon conversion, we already develop the new setup showing two prime part as a pure polymer matrix and ZnS:Cu single layer as shown in Fig. 3a. From this homemade setup, we clearly confirm the triboelectric effect of pure polymer matrices by means of the oscilloscope measurement under mechanical contact motion, which could show identical environment of stretching-releasing motion of ML process. We observed generated electric field (output voltage) for each polymer as following the trends: ER<PU<PDMS<EF<DS, proving the mechano-to-electro model. We then accessed electro-photon conversion model by means of this electric fields attributed to the pure polymer matrix under the mechanical motion. As shown in Fig. 3c, it has been demonstrated that a single layer of ZnS connected to a pure polymer matrix emits light under the influence of triboelectric fields generated by the pure polymer matrix. We re-emphasise that this evidence systematically demonstrates that the triboelectric-induced electroluminescence model can be validated at the single-particle level within the ML platform.

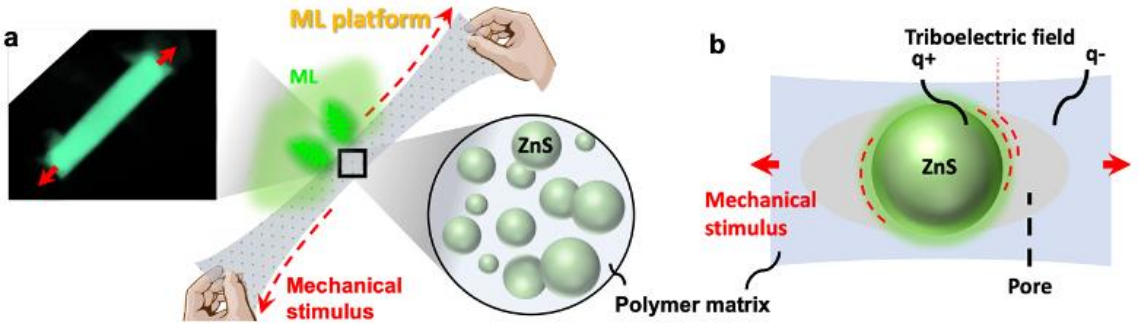

Fig. 1 a Schematic structure (inset: ML image under the stretching motion with human hands) **b** working process of the ML platform containing ZnS:Cu in the elastic polymer matrix.

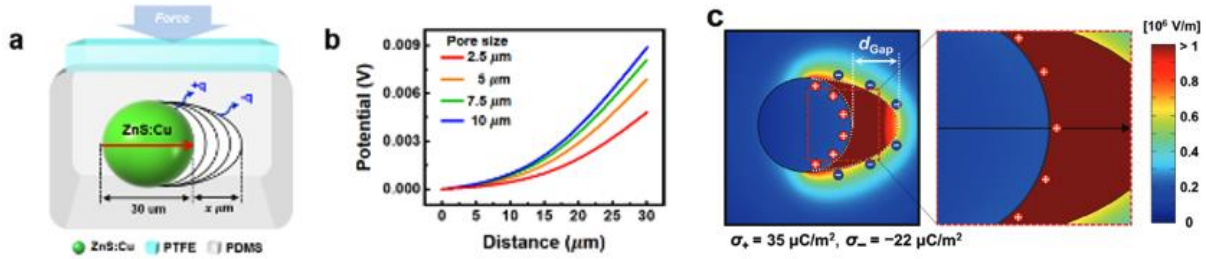

Fig. R7. a Schematic description of the pores that are formed between ZnS:Cu and PDMS by the external force. COMSOL simulation results: **b** numerically calculated output potential distribution. <*ACS Appl. Mater. Interfaces,* 2019, 11, 5200−5207> **c** Electric field inside a ZnS:Cu–PDMS composite with an interfacial gap on one side of the microparticle (area surroundedby a white dotted line) containing uniformly distributed triboelectric charges of opposite signs <*Small*, 2024, 20, 1613-6810>.

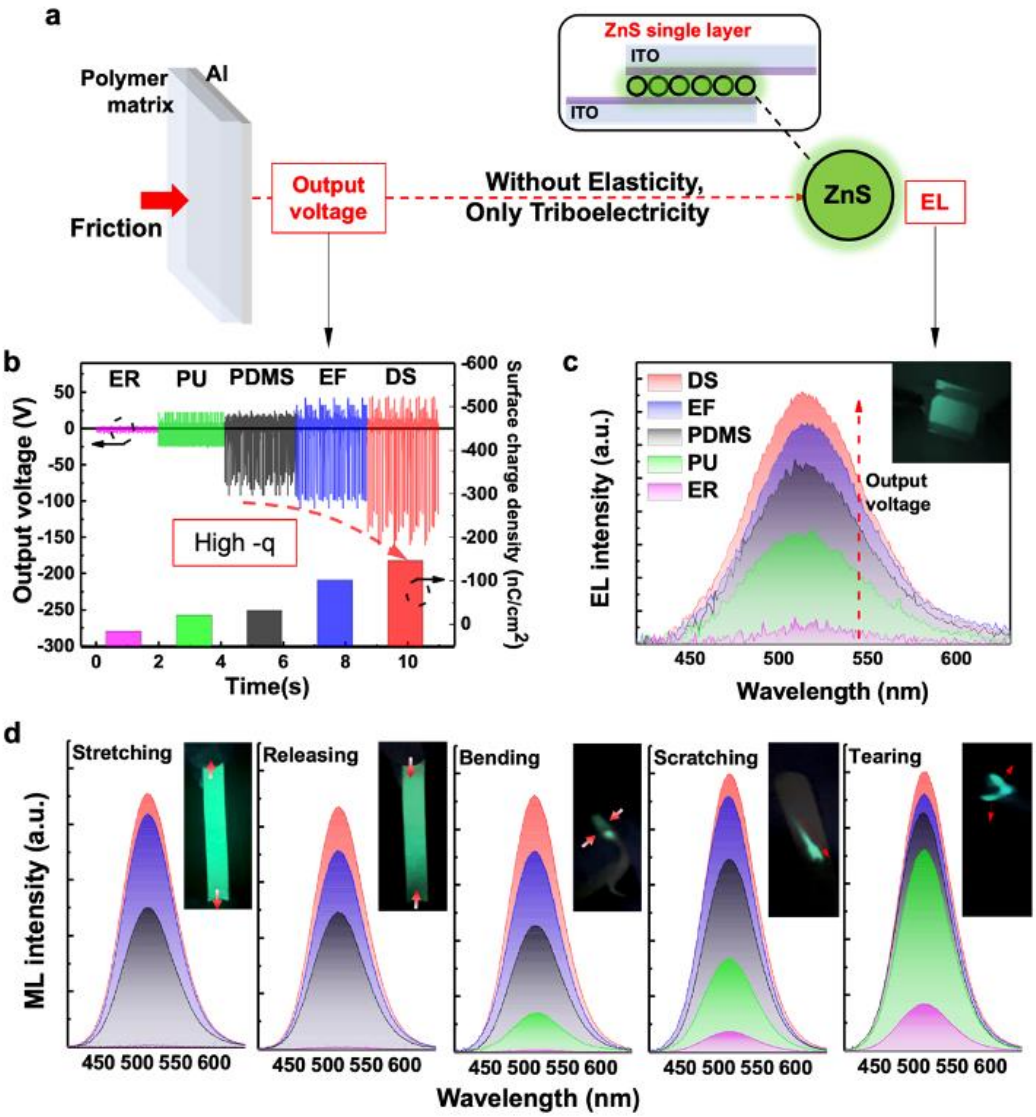

Fig. 3 | ML brightness depending on the triboelectricity of polymer matrix

a Home-made set-up for analysis AC-EL brightness of ZnS:Cu single layer attributed to independent triboelectricity of pure polymer matrices. **b** The output voltage and surface charge density of the polymer matrices. **c** AC-EL spectra of a ZnS:Cu single layer attributed to the output voltage of polymer matrices. Inset shows the AC-EL image of ZnS:Cu single layer attributed to output voltage of DS. **d** ML spectra according to the polymer matrices under the stretching, releasing, bending, scratching, and tearing, respectively. Inset images indicate the ML phenomenon under each mechanical motion.

→ Corresponding contexts in page 9, line 274.

"Based on these results, we then accessed oscilloscope analysis to verify the output voltage attributed to the surface triboelectricity of all polymer candidates. The latex glove is exploited

as an alternative material instead of ZnS:Cu surface (positive surface charge density +11 nC/cm^2) and apply tapping motion to generate triboelectric effect against with polymer interfaces. As shown in Fig. 3b, the trend of the output voltage follows the results of surface charge density from 10 V to 195 V with identical tendency of a series of all polymers, by means of triboelectric effect, which is likely to match with ML process. As expected, the trends of surface charge density are clearly proportional to the output voltage as an ability of triboelectric effect in polymers. Particularly, it is noteworthy that EF and DS (124 and 195 V) stand out here due to their highly negative triboelectricity compared to traditional PDMS (109 V), which leads us to expect remarkable luminescence performance."

Q2-3. The recoverability and intensity stability of ML in the inorganic–organic composites under continuous mechanical stimulus should be investigated.

A2-3. Thanks for the comment. As requested from Reviewer#2, we added the recoverability and intensity stability of the single fiber of ML textile sensor (corresponding to Fig. 5d-f) in Supplementary Fig. 22. We first assessed the stability of the ML intensity depending on the strain levels of 40%, 60%, and 90%, respectively, over the number of cycles ranging from 0 to 10,000. And the stretch-release frequency (deformation speed) was set to 100, 300, 700 cycles per minute (cpm) in all strain conditions. For the ER, we could not observe the stability of ML due to the sample fracture at all strain levels, which is ascribed to the low yield point (rigid property) of ER at 11%. In the case of 40% strain, PU, PDMS, EF, and DS exhibited superior stability up to 75% even after 10,000 cycles. Particularly, PDMS, EF, and DS maintained over 90% of their intensity, which may be due to their high-elastic nature of polymer matrix. However, the ML intensity of PU decreases with increasing frequency, indicating that low elasticity can lead to the rapid failure of recoverable properties of polymer under mechanical stimulus. Additionally, PU did not demonstrate stability at 60% and 90% strain regions owing to sample failure, which can be attributed to its low elasticity. In contrast, PDMS consistently showed outstanding ML stability at 40% and 60% strain region across all frequency, although the ML fiber sample was destroyed at 90% strain. However, EF and DS stood out for their high ML stability, maintaining over 90% intensity in all strain and frequency condition, made possible by their higher yield point compared with other candidates.

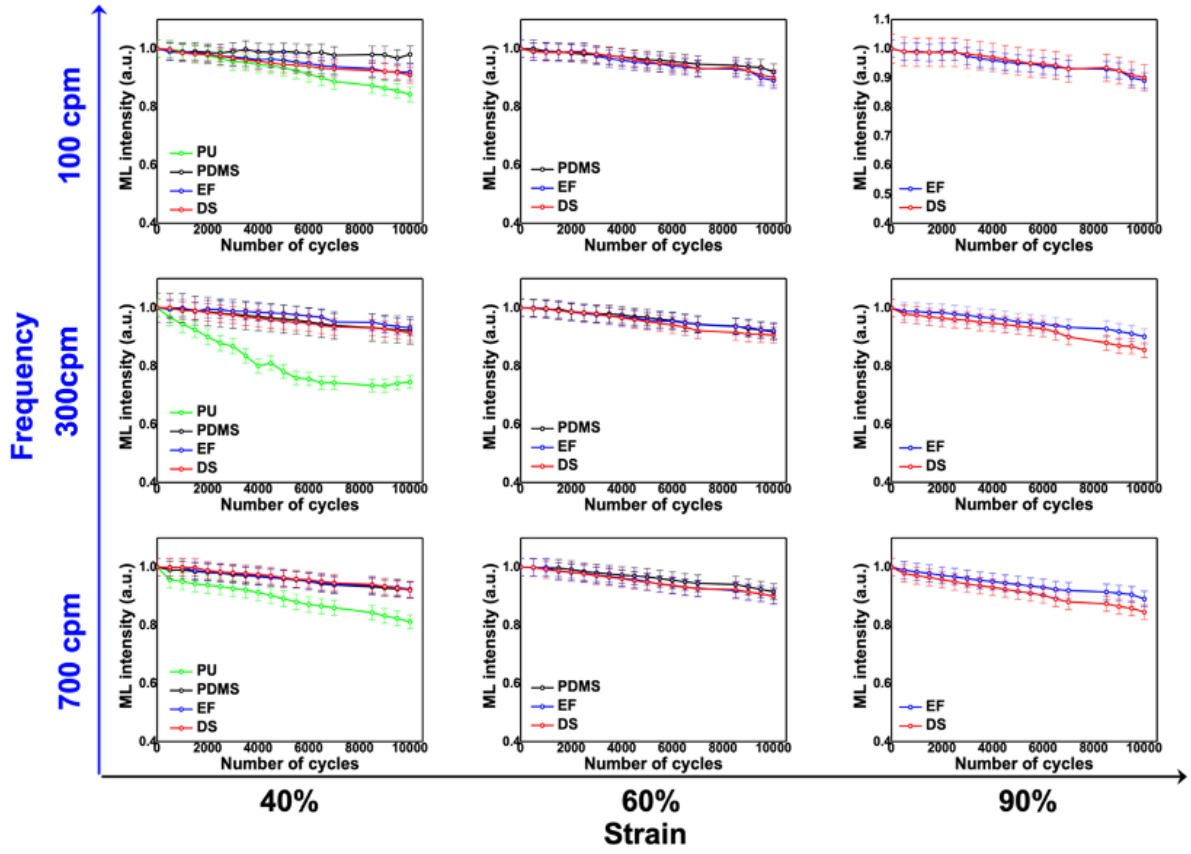

Supplementary Fig. 22. Stability test of the ML single fiber in continuous mechanical stimulus (number of cycles to 10,000), strain range (40%, 60%, 90% strain), and stretching-releasing frequency (deformation speed: 100, 300, 700 cpm), respectively.

→ Revised manuscript in page 12 and highlighted in yellow.

"To further verify the importance of polymer selection in this human motion detection sensor, we accessed the stability test for luminescent intensity of the ML fibers with polymer candidates ER, PU, PDMS, EF, and DS over the strain ranges of 40%, 60%, and 90%, respectively, up to 10,000 cycles (Supplementary Fig. 22). Since the stretching-releasing speed may cause the polymer to destroy, we also considered frequency of stretching releasing motion at 100, 300, and 700 cycles per minute (cpm) in all condition. In all tests, we do not observe the ML stability of ER due to sample fracture at all strain levels, attributed to its low yield point of 11%. At 40% strain as a lowest condition for stability test, PU, PDMS, EF, and DS showed superior stability up to 75% after 10,000 cycles, with PDMS, EF, and DS maintaining over 90% intensity due to their high elasticity. However, ML intensity of PU decreased with increasing frequency and failed to demonstrate stability at 60% and 90% strain due to its low elasticity. Furthermore, while PDMS does not show ML in 90% despite its superior stability as shown in 40% and 60%,

EF and DS stand for stability over the 90% across all strain and frequency condition. It proves again that elasticity of polymer is important factor in determining the stability performance to apply real wearable application.

Based on this fiber samples, we performed Commission Internationale de I'áclairge (CIE) colour coordinate measurements during the sitting-to-standing transition, which involves a strain range of 40% to 90%, to obtain the human motion signal from the ML textile on the knee."

Q2-4. The mechanical action frequency (i.e., deformation speed) could influence the ML intensity and the service life of composite materials. The dynamic aspects of the ML and the influence of frequency should be investigated.

A2-4. Thanks for the comment. As requested by Reviewer#2, we added a stability test of the single fiber of the ML textile sensor (corresponding to Fig. 5d-f) in Supplementary Fig. 22 in continuous mechanical stimulus (number of cycles to 10,000), strain range (40%, 60%, 90% strain), and stretching-releasing frequency (deformation speed: 100, 300, 700 cpm), respectively, and revised the manuscript in page 12.

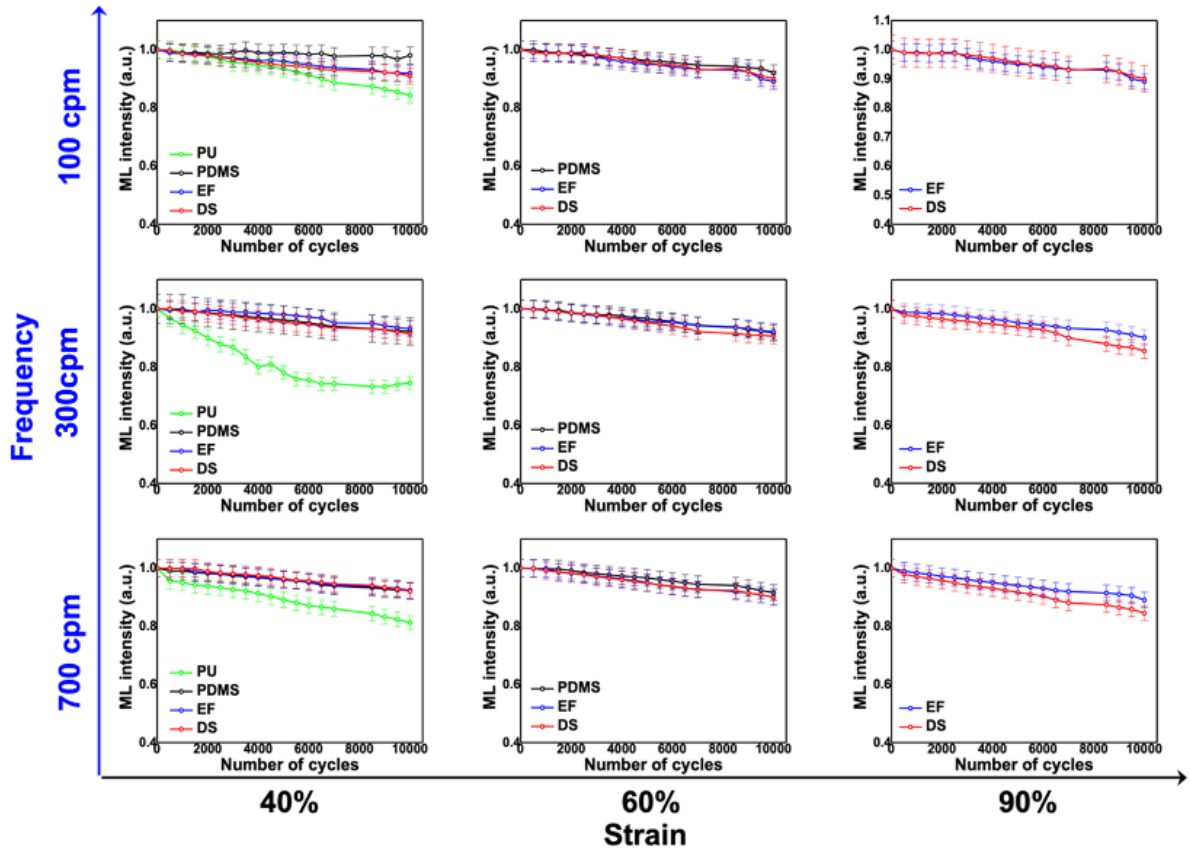

Supplementary Fig. 22. Stability test of the ML single fiber in continuous mechanical stimulus (number of cycles to 10,000), strain range (40%, 60%, 90% strain), and stretching-releasing frequency (deformation speed: 100, 300, 700 cpm), respectively.

→ Revised manuscript in page 12 and highlighted in yellow.

"To further verify the importance of polymer selection in this human motion detection sensor, we accessed the stability test for luminescent intensity of the ML fibers with polymer candidates ER, PU, PDMS, EF, and DS over the strain ranges of 40%, 60%, and 90%, respectively, up to 10,000 cycles (Supplementary Fig. 22). Since the stretching-releasing speed may cause the polymer to destroy, we also considered frequency of stretching releasing motion at 100, 300, and 700 cycles per minute (cpm) in all condition. In all tests, we do not observe the ML stability of ER due to sample fracture at all strain levels, attributed to its low yield point of 11%. At 40% strain as a lowest condition for stability test, PU, PDMS, EF, and DS showed superior stability up to 75% after 10,000 cycles, with PDMS, EF, and DS maintaining over 90% intensity due to their high elasticity. However, ML intensity of PU decreased with increasing frequency and failed to demonstrate stability at 60% and 90% strain due to its low elasticity. Furthermore, while PDMS does not show ML in 90% despite its superior stability as shown in 40% and 60%, EF and DS stand for stability over the 90% across all strain and frequency condition. It proves again that elasticity of polymer is important factor in determining the stability performance to apply real wearable application.

Based on this fiber samples, we performed Commission Internationale de I'áclairge (CIE) colour coordinate measurements during the sitting-to-standing transition, which involves a strain range of 40% to 90%, to obtain the human motion signal from the ML textile on the knee."

REVIEWERS' COMMENTS

Reviewer #1 (Remarks to the Author):

The authors have conducted comprehensive supplementary experiments and provided detailed responses to my previous questions, which are much appreciated. I am satisfied with most of the responses. However, I have one remaining suggestion regarding the statement: "observed charge density monotonically increases with the following trend: ER < PU < PDMS < EF < DS." In the revised text (lines 261–269), the authors attempted to explain this trend by attributing it to the electron affinity of nitrogen and oxygen atoms, as well as the polarity of ester groups. These explanations, however, do not appear to be convincing or scientifically robust. I recommend removing lines 261-269, as the proposed reasoning lacks sufficient evidence and rigor.

Reviewer #2 (Remarks to the Author):

publish as is.

<Point-by-Point Response to Reviewers' Comments>

Reviewer #1 (Remarks to the Author)

The authors have conducted comprehensive supplementary experiments and provided detailed responses to my previous questions, which are much appreciated. I am satisfied with most of the responses. However, I have one remaining suggestion regarding the statement: "observed charge density monotonically increases with the following trend: ER < PU < PDMS < EF < DS." In the revised text (lines 261–269), the authors attempted to explain this trend by attributing it to the electron affinity of nitrogen and oxygen atoms, as well as the polarity of ester groups. These explanations, however, do not appear to be convincing or scientifically robust. I recommend removing lines 261-269, as the proposed reasoning lacks sufficient evidence and rigor.

A1. Thank you for Reviewer#1's valuable comment. Based on the suggestion, we have removed the text from lines 261-269 regarding the electron affinity of nitrogen and oxygen atoms, as well as the polarity of ester groups, from our manuscript.

→ Removed corresponding contexts in Page 8 and 9.

To define the triboelectricity, we initially evaluated the surface charge density of all candidates, which contributes to the effective charge accumulation by mechanical action, capable of the triboelectric effect on the surface of polymer (Fig 3b). As a series of polymer matrices, the observed charge density monotonically increases with the following trend: ER < PU < PDMS < EF < DS (-15.9, -21.3, -31.9, -102.1, and -146.7 nC/cm^2), which could be attributed to the electron withdrawing ability of polymers in contacting surface (Supplementary Fig. 14). It is proved that all polymer candidates basically indicate the negatively charged surface potential by evidence with Kelvin probe force microscopy (KPFM), indicating identical trend with surface charge density (Supplementary Fig. 15). This strongly suggests that negatively charged polymer matrix can easily contribute the surface electron to alternative positively charged material to achieve the charge separation and accumulation for triboelectric effect. Based on these results, we then accessed oscilloscope analysis to verify the output voltage attributed to the surface triboelectricity of all polymer candidates. The latex glove is exploited as an alternative material instead of ZnS:Cu surface (positive surface charge density +11 nC/cm^2) and apply tapping motion to generate triboelectric effect against with polymer interfaces. As shown in Fig. 3b, the trend of the output voltage follows the results of surface charge density from 10 V to 195 V with identical tendency of a series of all polymers, by means of triboelectric effect, which is likely to match with ML process. As expected, the trends of surface charge density are clearly proportional to the output voltage

as an ability of triboelectric effect in polymers. Particularly, it is noteworthy that EF and DS (124 and 195 V) stand out here due to their highly negative triboelectricity compared to traditional PDMS (109 V), which leads us to expect remarkable luminescence performance.

Reviewer #2 (Remarks to the Author)

publish as is.

A1. Thanks for the Reviewer#2's positive review comment.